GEOPHYSICS, VOL. 63, NO. 1 (JANUARY-FEBRUARY 1998); P. 75–84, 16 FIGS.

Inversion of surface NMR data

Anatoly V. Legchenko* and Oleg A. Shushakov‡

ABSTRACT

The main advantage of the surface nuclear magnetic resonance (NMR) method compared to other geophysical methods in the field of groundwater investigation is the ability to measure an NMR signal directly from the water molecules. An NMR signal, stimulated by an alternating current pulse through an antenna at the surface, confirms the existence of water in the subsurface with a high degree of reliability. The NMR signal amplitude depends on the pulse parameter (the product of the pulse amplitude and its duration), bulk water volume, and water depth. Measurements are performed while varying the pulse parameter, and subsequent data processing reveals the number of water-saturated layers, and data concerning their depth, thickness, and water content.

One of the major problems in the practical application of the NMR method is the very weak signal (<3000 nV); hence the problem of signal to noise ratio (S/N). S/N can be improved by stacking the signal, but measurement time is increased. We have developed an algorithm that minimizes the number of measurements (number of different values of the pulse parameter) without a loss of inversion accuracy for a given S/N ratio, making it possible to determine a set of optimal pulses for the measurements.

NMR measurements are also sensitive to the electrical conductivity of the subsurface; an electrically conductive subsurface causes variations in the depth of investigation and In the vertical resolution of the method. Experience gained from application of the method has proven that both the inversion algorithm and the analysis of the problem are efficient.

INTRODUCTION

The main advantage of the surface NMR method, compared with other geophysical methods for water prospecting is that the surface measurement of the nuclear magnetic resonance (NMR) signal from water molecules in the subsurface ensures that it only responds to the subsurface water. Used routinely in Russia and tested in other countries (Schirov et al., 1991; Goldman et al., 1994; Lieblich et al., 1994) the method has demonstrated its potential.

Because the parameters of currently available surface NMR equipment, such as Hydroscope (ICKC, Russia) and NUMIS (IRIS Instruments, France), do not permit measurements of the very short signals (less then 30 ms) corresponding to "bounded" water in the subsurface, the vertical distribution of the water content deduced from the NMR data corresponds to the location and amount of "free" water in the aquifers. Free water distribution in the subsurface is a solution of integral equation and, like many other ill-posed problems, the inversion is sensitive to field measurement errors caused by external electromagnetic interferences such as electrical discharges in the atmosphere, magnetic storms, and all kinds of electrical currents through the subsurface. Interferences may also be caused by cultural noise produced by power lines, electrical generators and engines. In addition, the electrical conductivity of the subsurface (the operational frequency is between 1.5 and 2.8 kHz) not only attenuates the signal, but also has an effect on the kernel of the integral equation. Knowledge of this effect is important for the practical application of the method and for data interpretation.

Total time of field work, which is a matter of practical importance, depends largely on the number of measurements required for the extraction of the information from the noise-contaminated data. However, as the relaxation time of the NMR signal in water-saturated nonmagnetic rocks depends on the mean size of the pores and varies from tens to hundreds of milliseconds (Schirov et al., 1991), measurements cannot be repeated more frequently than every few seconds.

To minimize the field work time, we have developed an algorithm for optimizing the number of measurements based on an evaluation of the signal to noise ratio (S/N) using the Tikhonov regularization method for data inversion. We used computer simulation to estimate the performance of the NMR

Manuscript received by the Editor October 10, 1995; revised manuscript received April 25, 1997.
*BRGM-DR/GIG, 3, Avenue C. Guillemin-BP 6009, 45060 Orleans cedex 2, France. E-mail: a.legchenko@brgm.fr.
‡Russian Academy of Sciences, Institute of Chemical Kinetics and Combustion, 3, Institutskaya Street, Novosibirsk, 630090, Russia and Novosibirsk State University, Novosibirsk, Russia.

method over electrically conductive subsurface rocks. With a conductive half-space model, all calculations were performed using a circular 100 m diameter antenna, a vertical geomagnetic field with the magnitude of 58685.45 nT, and the corresponding Larmor frequency of protons in water $\omega_0/2\pi = 2500$ Hz. Natural noises (interference) were simulated by computer-generated random numbers.

THEORY

Quantitative determination of subsurface water

If V is the total volume of the subsurface, V_W is the part of the subsurface filled with water, and V_R is the part of the subsurface occupied by rocks, and we can write $V = V_W + V_R$. Assuming that the water (V_W) and rocks (V_R) are homogeneously distributed in the total volume V, we can use the volume per unit (for example, $V = 1$ m^3) instead of using the total volume of the subsurface. The water (V_W) in a porous medium can be divided into two parts: free water V_F (water which is unattached to grain walls and can be extracted from the rock) and bounded water V_B (water which is captured by grains and cannot be extracted). Thus, we also assume that $V_W = V_F + V_B$. These two parts of subsurface water are distinguished by a fundamental difference in the decay time between the NMR responses from free water and those from bounded water: the signal decay time generated by bounded water is much shorter. Although further research is required to establish a precise relationship between the decay times of the NMR signal and the hydrogeological parameters of water in a porous medium, our experience in NMR application allows us to assume, with sufficient accuracy, that the decay time for bounded water is less than 20–30 ms and for free water it is between 30 and 1000 ms. Parameters of surface NMR equipment currently available, such as Hydroscope (ICKC, Russia) and NUMIS (IRIS Instruments, France), do not permit measurements of the very short signals (less than 30 ms); hence we may say that only signals from the free water (V_F) are measured. Thus, we can tell that the water content is the part of the total volume of the subsurface occupied by the free water: $n = V_F/V$. For example, in a dry rock $n = 0$ and in a bulk water of a lake $n = 1$.

Surface NMR method

A wire antenna is laid out on the ground, normally in a circle with a diameter of between 10 and 200 m, depending on the depth of aquifers; it may also be laid out in a "figure of eight" to improve S/N ratio (Trushkin et al., 1994). The antenna is then energized by a pulse of alternating current

$$i(t) = I_0 \cos(\omega_0 t), \qquad 0 < t \le \tau, \tag{1}$$

where I_0 and τ are respectively the pulse amplitude and duration. The frequency of the current ω_0 is equal to the Larmor frequency of the protons in the geomagnetic field $\omega_0 = \gamma H_0$, with H_0 being the magnitude of the geomagnetic field and γ the gyromagnetic ratio for the protons (the physical constant).

The pulse causes precession of the protons around the geomagnetic field, which creates an alternating magnetic field that can be detected using the same antenna after the pulse is terminated (the free induction decay method). In practice, the NMR response recording is possible after an instrumental delay ("dead time"). The time diagram of the signal measurement process is depicted in Figure 1. Oscillating with the Larmor frequency, the NMR signal $e(t, q)$ has an exponential envelope and depends on the pulse parameter $q = I_0\tau$

$$e(t, q) = e_0(q) \exp(-t/T_2^*) \cos(\omega_0 t + \varphi_0), \tag{2}$$

where T_2^* is the spin-spin relaxation time, and φ_0 is the phase of the NMR signal.

The initial amplitude $e_0(q)$ can be calculated as (Trushkin et al., 1995):

$$e_0(q) = \omega_0 M_0 \int_V h_{1\perp} \sin\left(\frac{1}{2}\lambda h_{1\perp} q\right) n(\mathbf{r})\, dV(\mathbf{r}), \tag{3}$$

where M_0 is the nuclear magnetization for the protons, $h_{1\perp} = H_{1\perp}/I_0 = f(\mathbf{r}, \rho(\mathbf{r}), \alpha)$, with $H_{1\perp}$ being the transmitting magnetic field component perpendicular to the geomagnetic field, α the geomagnetic field inclination, $\rho(\mathbf{r})$ the subsurface resistivity, $0 \le n(\mathbf{r}) \le 1$ the water content, and $\mathbf{r} = r(x, y, z)$ the coordinate vector.

Assuming that stratification is horizontal and the vertical distribution of resistivity is known ($\rho(\mathbf{r}) = \rho(z)$), equation (3) of the signal amplitude e_0 can be simplified to a Fredholm linear integral equation of the first kind written as

$$e_0(q) = \int_0^L K(q, z) n(z)\, dz, \tag{4}$$

where

$$K(q, z) = \omega_0 M_0 \int_{x,y} h_{1\perp} \sin\left(\frac{1}{2}\gamma h_{1\perp} q\right) dx\, dy. \tag{5}$$

Numerical results show that the distant protons produce a negligibly small signal; hence we can limit integration by $x^2 + y^2 \le (2D)^2$ and $L = 2D$, where D is the antenna diameter.

An example of the NMR signal ($e_0(q)$), calculated for a 5-m-thick layer of bulk water ($n = 1$) situated at various depths in the nonconductive half-space, demonstrates the method's capability of determining a subsurface water location caused by the distinct differences in the shape of the signal (Figure 2). Results of NMR signal modeling over a conductive subsurface are also given in Shushakov (1996).

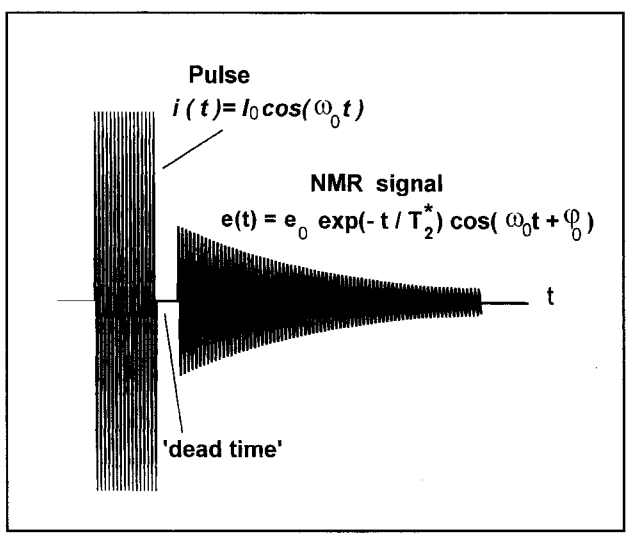

FIG. 1. Time diagram of the NMR signal measurements.

Variation of the geomagnetic field also causes the NMR signal to vary (Trushkin et al., 1993). Here, however, we assume the geomagnetic field to be homogeneous over the whole volume and unchanged during the measurements.

Inversion algorithm

The vertical distribution of water content $n(z)$ is resolved by equation (4). This linear equation may be solved by projecting it onto finite-dimensional subspace, and approximated by the projected equation

$$\sum_j \phi_j(q_i) n_j = e_{0i}, \tag{6}$$

where $i = 1, 2, \ldots, I$, $j = 1, 2, \ldots, J$, and $\phi_j(q)$ is a set of kernel vectors obtained by projecting the kernel $K(q, z)$ on a set of basis functions $b_j(z)$, so that

$$n(z) = \sum_j n_j b_j(z), \tag{7}$$

and

$$\phi_j(q) = \int_0^L K(q, z) b_j(z)\, dz. \tag{8}$$

From a physical point of view, the problem allows the basis functions to be assumed as box-car functions. Hence, the kernel vectors are the elementary responses from the layers of water ($n_j = 1$), characterized by their depth z and thickness Δz. When the depth intervals are

$$0 \le z \le L, \qquad \Delta z_j = z_{j+1} - z_j, \qquad L = \sum_{j=1}^{J} \Delta z_j, \tag{9}$$

the basis functions are

$$b_j(z_j \le z < z_{j+1}) = 1, \qquad b_j(z < z_j, \quad z \ge z_{j+1}) = 0, \tag{10}$$

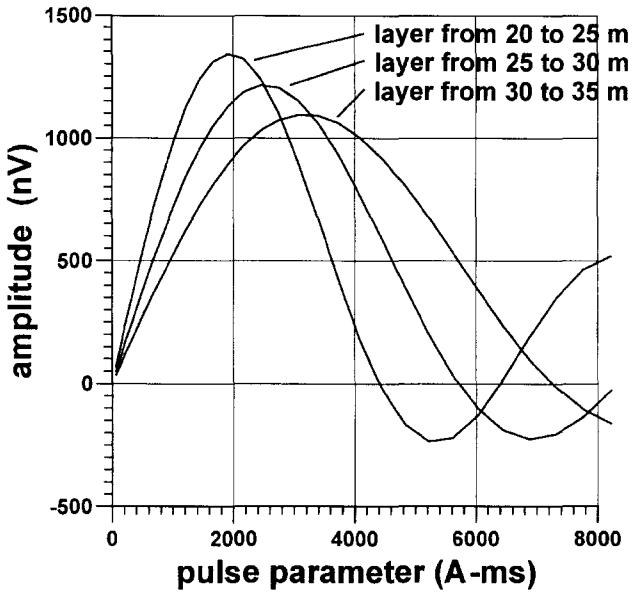

FIG. 2. Initial amplitude of the NMR signal versus pulse parameter, calculated for a 5-m-thick layer of bulk water situated at the depths of 20, 25, and 30 m.

and the kernel vectors are

$$\phi_j(q) = \int_{z_j}^{z_{j+1}} K(q, z)\, dz. \tag{11}$$

The vertical resolution of the method depends on the magnetic field created by the antenna; the larger the gradient of the field, the better the resolution. The magnetic field of the circular antenna with a current passing through is well known; the gradient of the field is large closer to the surface and decreases with increasing depth. Consequently, the resolution of the NMR is also better closer to the surface. The vertical resolution corresponds to thicknesses of the basis functions, and hence,

$$\Delta z_1 \le \Delta z_2 \le \cdots \le \Delta z_j \le \cdots \le \Delta z_J. \tag{12}$$

In a matrix notation, projected equation (6) can be written as

$$\underset{\sim}{\mathbf{A}}\mathbf{n} = \mathbf{e}_0, \tag{13}$$

where $\underset{\sim}{\mathbf{A}} + [a_{i,j}]$ is a rectangular matrix of $I \times J$ with the elements $a_{i,j} = \phi_j(q_i)$; $\mathbf{e}_0 = (e_{01}, e_{02}, \ldots, e_{0i}, e_{0I})^T$, $e_{0i} = e_0(q_i)$ being the set of experimental data; and $\mathbf{n} = (n_1, n_2, \ldots, n_j, \ldots, n_J)^T$, $n_j = n(\Delta z_j)$ being the vertical distribution of water content, and the symbol T denoting transposition.

Numerical solution of matrix equation (13) is highly dependent on the choice of basis functions. For a unique and stable solution, the kernel vectors must be linearly independent. In this case, the number of the basis functions is small and, in spite of the uniqueness, such a solution has no practical importance because of a large discretization error. Increasing the number of basis functions reduces the error resulting from discretization, but the stability of the solution suffers because of the ill-conditioning of the problem. To establish a rule for determining the number of basis functions, we use the linear algebra definition: the matrix $\underset{\sim}{\mathbf{A}}$ is singular if the homogeneous system

$$\underset{\sim}{\mathbf{A}}\mathbf{v} = 0, \tag{14}$$

has a nontrivial solution. This means that some of the columns (or lines) of matrix $\underset{\sim}{\mathbf{A}}$ are linearly dependent.

If system (14) does not have a nontrivial solution, we can write

$$\underset{\sim}{\mathbf{A}}\mathbf{v} = \mathbf{g}, \tag{15}$$

where $\mathbf{v} = (v_1, v_2, \ldots, v_j, \ldots, v_J)^T$ is still an undefined vector, and $\mathbf{g} = (g_1, g_2, \ldots, g_i, \ldots, g_I)^T$ is the linear combination vector. From a practical point of view, it is important to not only know whether the vector $\mathbf{g} = 0$, but also how close it may be to zero. For this purpose, we may estimate the square norm of the vector $\mathbf{g}$ given by the quadratic expression

$$\mathbf{v}^T \underset{\sim}{\mathbf{C}}\mathbf{v} = |\mathbf{g}|^2, \tag{16}$$

where

$$\underset{\sim}{\mathbf{C}} = \underset{\sim}{\mathbf{A}}^T \underset{\sim}{\mathbf{A}}. \tag{17}$$

If there are kernel vectors that are not mutually independent, there are also the vectors $\mathbf{v}$, which make the square norm of the linear combination small, $|\mathbf{g}|^2 \to 0$. The extrema of the quadratic expression (16) are known from matrix theory, and are given if the previously introduced vectors $\mathbf{v}$ are the eigenvectors of the matrix $\underset{\sim}{\mathbf{C}}$. The values of the expression at the

extrema are the eigenvalues of $\underset{\sim}{\mathbf{C}}$, corresponding to selected eigenvectors. This can be written as

$$\underset{\sim}{\mathbf{V}}^T \underset{\sim}{\mathbf{C}}\, \underset{\sim}{\mathbf{V}} = \Lambda, \tag{18}$$

where $\underset{\sim}{\mathbf{V}} = [v_{i,j}]$ is the matrix of eigenvectors, and Λ is the diagonal matrix of eigenvalues of the matrix $\underset{\sim}{\mathbf{C}}$ with the elements λ_j.

Stability of the matrix $\underset{\sim}{\mathbf{C}}$ can be estimated using the concept of condition number

$$cond(\underset{\sim}{\mathbf{C}}) = (\lambda_{\max}/\lambda_{\min}) \geq 1, \tag{19}$$

where $\lambda_{\max}$, $\lambda_{\min}$ are the maximum and minimum eigenvalues of the matrix $\underset{\sim}{\mathbf{C}}$. In general, a linear system with a small condition-number value is more stable than a system with a large one.

For a finite, positive-definite matrix $\underset{\sim}{\mathbf{C}}$, the largest eigenvalue is

$$\lambda_{\max} < \sum_j \lambda_j = \sum_j c_{jj} = Tr\,(\underset{\sim}{\mathbf{C}}), \tag{20}$$

where c_{jj} are the diagonal elements of the matrix $\underset{\sim}{\mathbf{C}}$. These diagonal elements (c_{jj}) are finite-real numbers and they depend mainly on the scaling of the problem. Consequently, $\lambda_{\max}$ depends also on the scaling, and the linear dependence of the kernel vectors does not have much of an effect on $\lambda_{\max}$. However, $\lambda_{\min} = |\mathbf{g}|^2_{\min}$ is the square norm of the linear combination vector and may be negligibly small with the same scaling if some of the kernel vectors are linearly dependent. Hence, if some of the kernel vectors are not linearly independent, then $\lambda_{\min} \to 0$, $\lambda_{\max} \approx const$, and $cond(\underset{\sim}{\mathbf{C}}) \to \infty$, and the solution becomes unstable. Thus, by varying the linear dependence between the kernel vectors we can influence the stability of the solution.

The linear dependence between any two vectors can be estimated using the correlation coefficient between them

$$r_{j,k} = \frac{\int \phi_j(q)\phi_k(q)\,dq}{\sqrt{\int \phi_j^2(q)\,dq \int \phi_k^2(q)\,dq}}. \tag{21}$$

When the vectors are linearly dependent, $abs(r_{j,k}) \to 1$. The kernel vectors $\phi_j(q_i)$ also are the columns of the matrix $\underset{\sim}{\mathbf{A}}(a_{i,j} = \phi_j(q_i))$, and the correlation coefficient between two of them is

$$r_{j,k} = \frac{\sum_{i=1}^{I} a_{i,j} a_{i,k}}{\sqrt{\sum_{i=1}^{I} a_{i,j}^2 \sum_{i=1}^{I} a_{i,k}^2}}, \tag{22}$$

where $a_{i,j}$, $a_{i,k}$ are elements of the j and k columns of the matrix $\underset{\sim}{\mathbf{A}}$.

Now we can express the matrix of the correlation coefficients as

$$\underset{\sim}{\mathbf{R}} = \underset{\sim}{\mathbf{D}}\,\underset{\sim}{\mathbf{C}}\,\underset{\sim}{\mathbf{D}}, \tag{23}$$

where $\underset{\sim}{\mathbf{R}} = [r_{j,k}]$ is a matrix of $J \times K$, $J = K$, the elements $r_{j,k} = r_{k,j}$ are the correlation coefficients between the j and k columns of the matrix $\underset{\sim}{\mathbf{A}}$, and $\underset{\sim}{\mathbf{D}}$ is the diagonal matrix with the elements

$$d_{j,j} = 1 \Big/ \sqrt{\sum_i a_{i,j}^2}. \tag{24}$$

Thus, when the kernel vectors are not linearly independent $abs(r_{j,k}) \to 1$ and $cond(\underset{\sim}{\mathbf{C}}) \to \infty$. So, the correlation coefficient between the two most linearly dependent kernel vectors can be used for the matrix stability evaluation. For L_2 norm, $cond\,(\underset{\sim}{\mathbf{A}}) = \sqrt{cond(\underset{\sim}{\mathbf{C}})}$; hence, the linear dependence between the kernel vectors affects not only the stability of the matrix $\underset{\sim}{\mathbf{C}}$ but also the stability of the matrix $\underset{\sim}{\mathbf{A}}$.

The kernel vectors $\phi_j(q)$ can be calculated for various depths z_j and thicknesses Δz_j of the basis functions. These vectors depend on the vertical gradient of the magnetic field of the antenna. The greater the difference between z_j and z_k, the more $\phi_j(q)$ and $\phi_k(q)$ are linearly independent because of a greater difference in the antenna magnetic field at these two depths. If the columns of the matrix $\underset{\sim}{\mathbf{A}}$ correspond to the kernel vectors arranged by increasing depth. Then, taking into account thickness condition (12), we can write

$$r_{j,j} = 1, \qquad r_{j,j-2} < r_{j,j-1} < r_{j,j}, \qquad r_{j,j+2} < r_{j,j+1} < r_{j,j}. \tag{25}$$

This relationship between the correlation coefficients, based on knowledge of the physical property of the problem, can be illustrated by two numerical examples:

1) The depth interval between 0 and 100 m is divided into layers of equal thickness $\Delta z_j = 1$ m. The correlation coefficient, equation (22), was calculated between the layer situated at different fixed depths and all the other layers (Figure 3). The depth of a layer was taken as the depth to the top of that layer. As was expected for layers of equal thickness, the farther apart the layers, the more they are linearly independent.
2) Calculations were performed for a layer with $\Delta z_j = 1$ m, situated at different fixed depths and another layer at the same depth, but with variable thickness (Figure 4). The larger the differences in thickness between the layers, the more they are linearly independent.

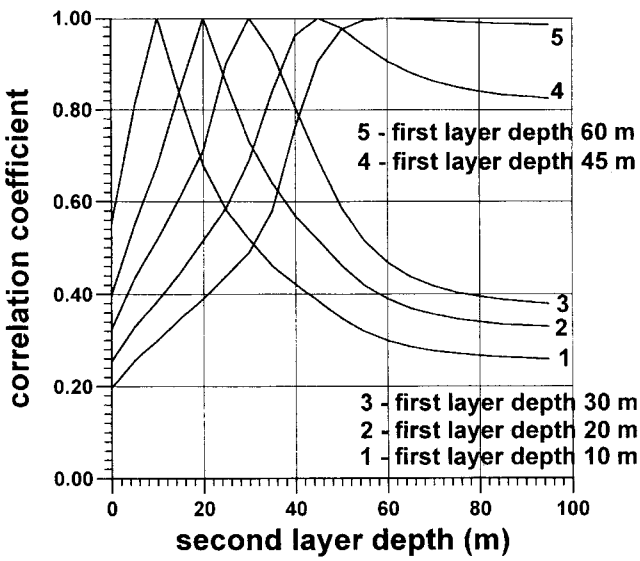

FIG. 3. The correlation coefficient between two signals from 1-m-thick water layers. One layer is held at fixed depths (top of the layer) of 10, 20, 30, 45, and 60 m, respectively, while the depth of the top of the other layer varies.

So, by varying both z_j and Δz_j it is possible to acquire sets of kernel vectors with an expected linear dependence.

We can define the parameter for the discretization of the integral equation as the correlation coefficient between two successive kernel vectors $\phi_j(q)$ and $\phi_{j+1}(q)$, which have a physical sense of the NMR signals from the water layers, situated at neighboring depths. For the matrix $\underset{\sim}{\mathbf{A}}$, it is the correlation coefficient between the j and $j+1$ columns: $r_{1,2} = r_{2,3} = \cdots = r_{j,j+1} = \cdots = r_{J-1,J} = R$. Discretization with parameter R allows us to determine the maximum number of basis functions with homogeneously distributed linear dependence. When R is fixed, the number of the basis functions J with the depth z_j and the thickness Δz_j for each one is also fixed. We are also sure that the correlation coefficient between any two columns (the kernel vectors) is not more than R. By varying R, it is possible to manage the condition number of the matrix $\underset{\sim}{\mathbf{A}}$. The matrix $\underset{\sim}{\mathbf{R}}$ for this special case is symmetric and diagonally dominant

$$\underset{\sim}{\mathbf{R}} = \begin{bmatrix} 1 & R & r_{1,3} & \cdot & r_{1,k} & \cdot & \cdot & r_{1,K} \\ R & 1 & R & \cdot & r_{2,k} & \cdot & \cdot & r_{2,K} \\ r_{3,1} & R & 1 & \cdot & \cdot & \cdot & \cdot & \cdot \\ \cdot & \cdot & R & \cdot & R & \cdot & \cdot & \cdot \\ r_{j,1} & r_{j,2} & \cdot & \cdot & 1 & \cdot & \cdot & r_{j,K} \\ \cdot & \cdot & \cdot & \cdot & R & \cdot & R & \cdot \\ \cdot & \cdot & \cdot & \cdot & \cdot & \cdot & 1 & R \\ r_{J,1} & r_{J,2} & \cdot & \cdot & r_{J,k} & \cdot & R & 1 \end{bmatrix}. \quad (26)$$

From the matrix $\underset{\sim}{\mathbf{R}}$ we can conclude that either of the two neighboring elements of the solution n_j, n_{j+1} are equally vulnerable to noise, and can be accurately found only when the parameter of discretization R is accorded with experimental errors so that R becomes smaller as the errors become larger ($0 \le abs(R) \le 1$). When the errors and R stay unchanged, well-separated elements can be resolved with higher accuracy then neighboring ones. Practically, this means that boundaries of water-saturated subsurface layers are always determined with a lower accuracy than those of two layers that are well separated by depth. More information regarding the application of the matrix of the correlation coefficients for linear problem analysis can be found in Tarantola (1987).

Numerical calculations of the condition number of the matrix $\underset{\sim}{\mathbf{A}}$ versus the correlation coefficient R (Figure 5) confirm the existence of the relationship between the two parameters. The eigenvalues were calculated by the standard Jacobi method (Stoer and Bulirsch, 1980) for $\underset{\sim}{\mathbf{C}} = \underset{\sim}{\mathbf{A}}^T\underset{\sim}{\mathbf{A}}$ matrix and afterwards, as $cond(\mathbf{A}) = \sqrt{cond(\underset{\sim}{\mathbf{A}}^T\underset{\sim}{\mathbf{A}})}$, for $\underset{\sim}{\mathbf{A}}$ itself. To calculate the elements of the matrix $\underset{\sim}{\mathbf{A}}$, we assume equal thicknesses $\Delta z = \Delta z_1 = \Delta z_2$ for the kernel vectors and their depths $(z_j + \Delta z_j/2)$. By varying Δz, we calculate $\phi_1(q)$, $\phi_2(q)$ so that $r_{1,2} = R$. Subsequently, all layers that follow and their related kernel vectors $\phi_j(q)$ can be deduced easily by varying Δz_j [taking into account thickness condition (12)] to get $r_{j-1,j} = R$.

The condition number of the matrix $\underset{\sim}{\mathbf{A}}$ can be used for estimating the relative error amplification

$$\sqrt{(|\delta n(z)|^2/|n(z)|^2)} \le cond(\underset{\sim}{\mathbf{A}})\sqrt{(|\varepsilon(q)|^2/|e_0(q)|^2)}, \quad (27)$$

where $|\varepsilon(q)|^2$ is the experimental data error, $|e_0(q)|^2$ is the signal, $|\delta n(z)|^2$ is the error of the solution, and $|n(z)|^2$ is the solution itself. The condition number is the less optimistic evaluation of the error amplification. Meanwhile, for determining the reasonable number of basis functions, it is also possible to employ the average relative error amplification, as proposed by Twomey (1974)

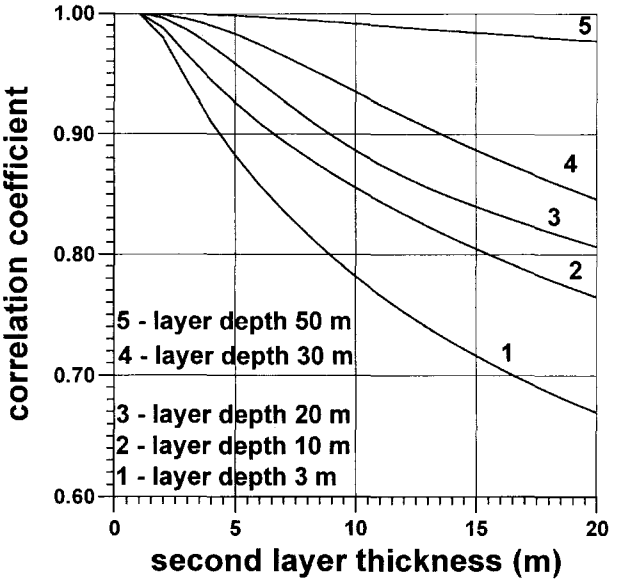

FIG. 4. Correlation coefficient between two NMR signals. One signal is from a 1-m-thick water layer, located at depths (top of the layer) of 3, 10, 20, 30, and 50 m respectively, and the other signal is from a water layer located at the same depth (top of the layer), but with varying thickness.

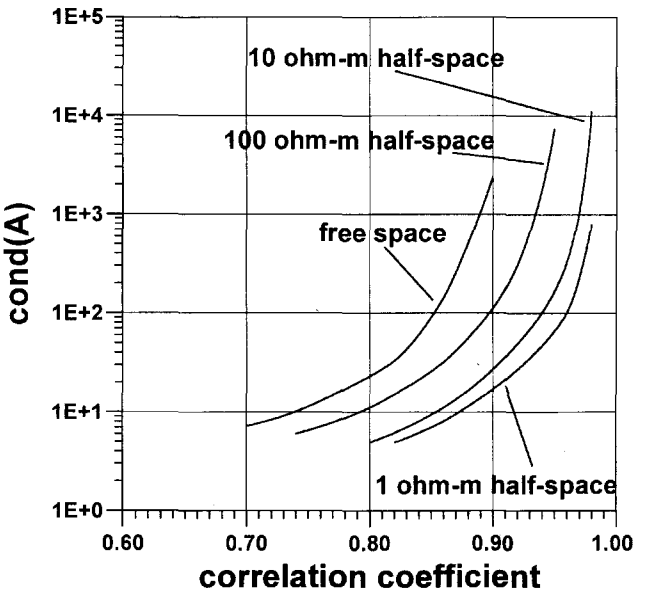

FIG. 5. Relationship between the condition number of the matrix $\underset{\sim}{\mathbf{A}}$ and the correlation coefficient R as a function of half-space resistivity.

$$k_\varepsilon = \sqrt{(|\delta n(z)|^2/|n(z)|^2)}\Big/\sqrt{(|\varepsilon(q)|^2/|e_0(q)|^2)}$$

$$= \frac{1}{J}\sqrt{\sum_{j=1}^{J}(1/\lambda_j)\sum_{j=1}^{J}\lambda_j}, \qquad (28)$$

where λ_j is the eigenvalues of the matrix $\underset{\sim}{\mathbf{C}}$. The general nature of the result will be unchanged if the criteria are varied, but based on numerical results and practical experience, we use criteria given by equation (28).

The average relative error amplification can be calculated for various values of the correlation coefficient R (Figure 6). There is a relationship between the two parameters, that is quite similar to the one in Figure 5.

We prescribe the relative error of the solution to be $\sqrt{(|\delta n(z)|^2/|n(z)|^2)} = 1$, and assume that this represents a limit where the solution is still reliable. The relative error of the data $\sqrt{(|\varepsilon(q)|^2/|e_0(q)|^2)}$ can be evaluated before the measuring is started. It does not take much time, because the number of measurements for this evaluation can be much smaller than the number of measurements required for inversion. We also assume that the average noise magnitude remains fairly constant during the measuring time, and that it is independent of the pulse parameter. Thus it can be expressed

$$k_\varepsilon = \sqrt{|e_0(q)|^2/|\varepsilon(q)|^2} = S/N. \qquad (29)$$

Knowing S/N, we can find k_ε and subsequently R using the graph depicted in Figure 6. When the basis functions (and hence the kernel vectors) have been determined, the number of measurements may be taken as the same ($I = J$). The values of q can be selected so that the signal is measured by the pulse parameter values corresponding to maximums of the kernel vectors (Figure 7). Some of the kernel vectors are shown in Figure 2, and their maximums are clearly distinguished. Figure 7 shows the relationship between the mean depth of the basis function ($z_j + \Delta z_j/2$) and the pulse parameter value q_{em}, by which the kernel vector is maximum ($\phi_{j\max} = \phi_j(q_{emj})$). This relationship leads to the determination of the values of the pulse parameter $q_i = q_{emj}$.

Discretization carried out with the correlation coefficient R as a parameter, taking into account S/N evaluation, allows determination of the reasonable minimum number of measurements. It also enables estimation of the vertical resolution for a given S/N because of the existing relationship between the correlation coefficient and the thickness of the basis function. The example of this relationship in Figure 8, calculated for the free-space model, numerically demonstrates the general idea that vertical resolution drops at greater

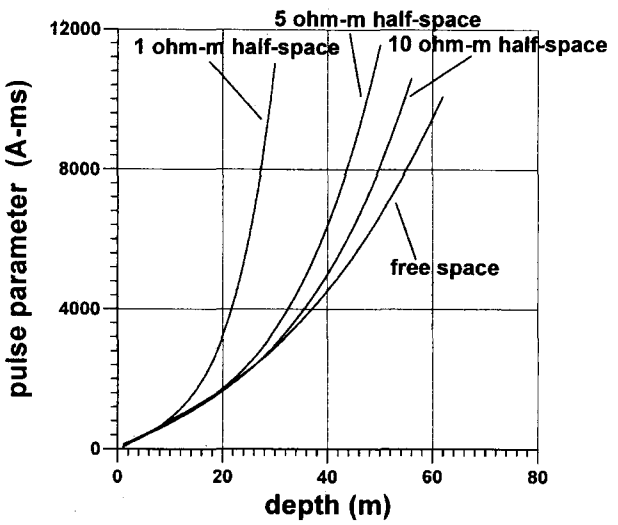

FIG. 7. Relationship between the mean depth of the water-saturated layer ($z_j + \Delta z_j/2$) and the pulse parameter at the NMR response maximum (i.e., $\phi_{j\max} = \phi_j(q_{emj})$).

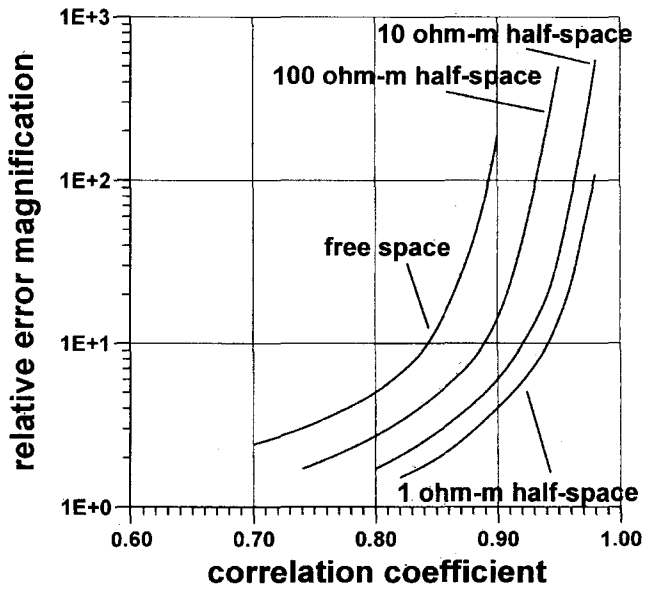

FIG. 6. Average relative error amplification versus correlation coefficient R, calculated for models with various half-space resistivity.

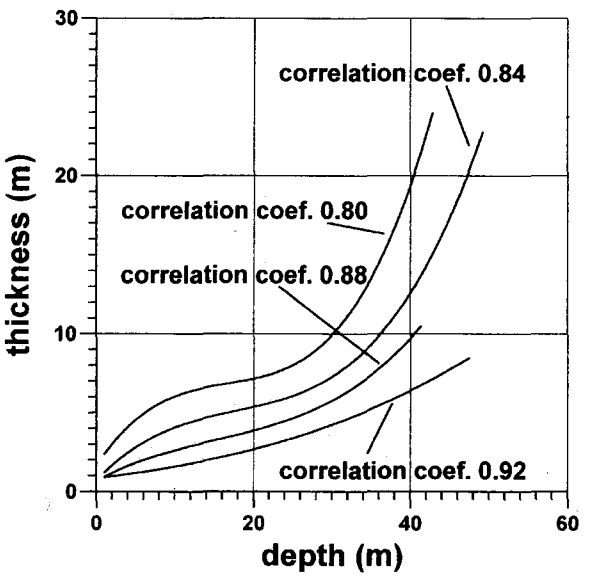

FIG. 8. The thickness of the j model layer (Δz_j) versus its mean depth ($z_j + \Delta z_j/2$) for various R calculated using the free-space model.

depths. Resolution also depends on S/N, because smaller R values correspond to smaller S/N values.

We can also compare the vertical resolution for half-space models of various electrical resistivity (Figure 9). Calculations were performed with $k_\varepsilon \approx 100$ for each one to eliminate S/N influence and demonstrate only the effect of electrical conductivity. For electroconductive models, the results reveal better resolution close to the surface. This can be explained by a more abrupt change of the antenna magnetic field in a conductive medium. The screening effect, which induces a decrease in the depth of the investigation limit, is demonstrated in Figure 10, where the depth of the top of a 1-m-thick water layer ($n = 1$)

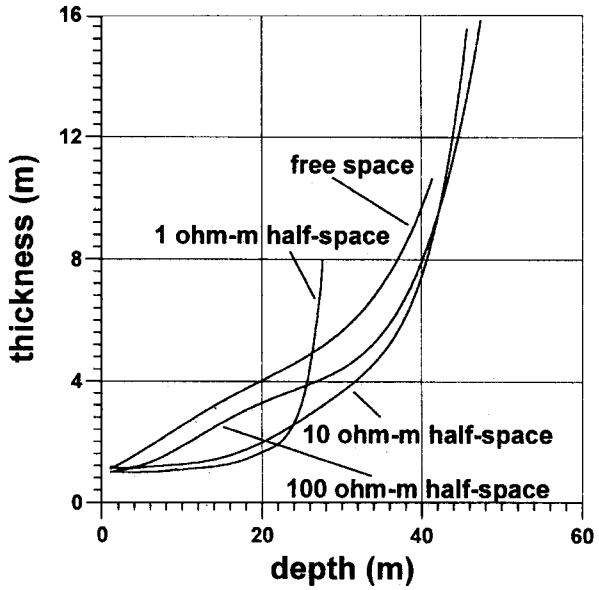

FIG. 9. The thickness of the j model layer (Δz_j) versus its mean depth ($z_j + \Delta z_j/2$), calculated using various half-space resistivity models with average relative error amplification $k_\varepsilon = 100$.

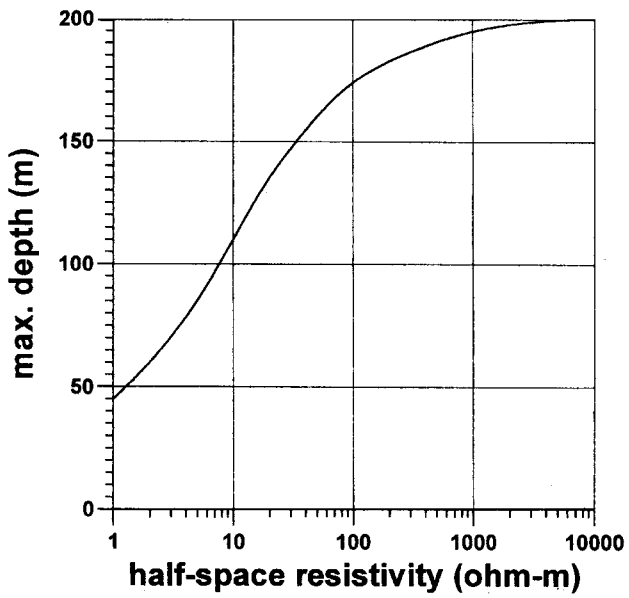

FIG. 10. The maximum depth detection for a 1-m-thick bulk water layer versus the resistivity of the half-space.

is depicted versus the half-space resistivity. The depth was calculated to obtain the maximum initial amplitude of the NMR signal ($q = q_{em} \leq 12\,000$ A-ms), here equal to 25 nV, which is assumed to be the limit of instrumental sensitivity. We may conclude from Figures 9 and 10 that the influence of electrical conductivity is highly important when the half-space resistivity is less than 10 ohm-m, but that it is considerably less for values greater than 100 ohm-m.

The inversion was carried out according to the well-known Tikhonov regularization method (Tikhonov and Arsenin, 1977). To find an approximate solution of the matrix equation (13), this method supposes minimization of the Tikhonov functional

$$M_\eta(n) = \|\underset{\sim}{\mathbf{A}}\,\underset{\sim}{\mathbf{N}}_\eta - \mathbf{e}_{0\varepsilon}\|_{L_2} + \eta\|\underset{\sim}{\mathbf{N}}_\eta\|_{L_2} = \min, \qquad (30)$$

where the matrix $\underset{\sim}{\mathbf{A}}$ is a product of the initial linear integral equation (4) discretization, $\mathbf{e}_{0\varepsilon}$ is the vector of the experimental data contaminated by the noise $\varepsilon = \|\varepsilon\|_{L_2}$, $\underset{\sim}{\mathbf{N}}_\eta$ is the solution vector that minimizes the Tikhonov functional (30), and $\eta > 0$ is the parameter of regularization.

To solve this minimization problem, we followed the discrepancy principle introduced in Morozov (1966), which is based on the fact that for erroneous data, it does not make much sense to have the residual $\|\underset{\sim}{\mathbf{A}}\underset{\sim}{\mathbf{N}}_\eta - \mathbf{e}_{0\varepsilon}\|_{L_2}$ smaller than the experimental error. Hence, for a given $\varepsilon > 0$, we need to find a solution with a residual $\|\underset{\sim}{\mathbf{A}}\underset{\sim}{\mathbf{N}}_\eta - \mathbf{e}_{0\varepsilon}\|_{L_2} \leq \varepsilon$ and stabilize it by making $\|\underset{\sim}{\mathbf{N}}_\eta\|_{L_2}$ small. $\underset{\sim}{\mathbf{N}}_\eta$ is an approximation of the solution of matrix equation (13). When $\varepsilon \to 0$, $\eta(\varepsilon) \to 0$ and $\underset{\sim}{\mathbf{N}}_\eta \to \underset{\sim}{\mathbf{N}}$. For the optimization itself, we used the conjugate gradient method (Stoer and Bulirsch, 1980).

We are now in a position to summarise the points discussed above in an algorithm for the measurement and inversion of surface NMR data. The steps for the proposed algorithm are enumerated below:

1) Measure the noise and evaluate $N = \|\varepsilon\|_{L_2}$.
2) Using a few values of the pulse parameter q, estimate the average level of the NMR signal $S = \|e_0\|_{L_2}$.
3) Compute the average relative error amplification $k_\varepsilon = S/N$.
4) Use the relationship between the correlation coefficient and the error amplification $k_\varepsilon = k_\varepsilon(R)$, calculated in advance, to find the correlation coefficient R between the kernel vectors for the given k_ε.
5) Calculate the kernel vectors with the given R.
6) Assuming that the number of measurements is equal to the number of the basis functions, select pulse parameter values so that $q_i = q_{emj}$.
7) Using the noise evaluation ε, minimize the Tikhonov functional (30). The vector $\underset{\sim}{\mathbf{N}}_\eta$ is an approximation of the solution of the initial integral equation (4).

RESULTS AND DISCUSSION

Synthetic data inversion

To numerically demonstrate the performance of the proposed inversion algorithm, we used a two-layer model consisting of two 10-m-thick horizontal, homogeneous, infinite

water-saturated layers situated in free space at depths of 10 and 30 m, respectively. The water content of each layer was taken to be equal to 0.2 ($n = 0.2$), corresponding to 20% of free water, and the Larmor frequency was assumed to be equal to $\omega_0/2\pi = 2500$ Hz. A 100-m-diameter circular antenna was used to calculate the NMR signal. Experimental errors were simulated by adding zero mean random noise to the model data.

The inversion results are presented in Figure 11. Using knowledge of the S/N, an optimal number of the basis functions (J) and hence a minimal number of the measurements ($I = J$) were determined using the correlation coefficient R. This solution (thin solid line) fits the model quite well (dashed line) when S/N = 100. However, when S/N = 2, the fit to the model is very poor. Increasing the number of measurements does not improve the solution for a given S/N significantly, and to demonstrate this, inversion was also performed using a larger number both of the basis functions ($R = 0.94$, $J = 24$) and of measurements ($I = 32$). The solution is shown by the thick solid line. For practical purposes, the two solutions for each value of S/N are similar. However, the number of measurements, and hence the measurement time, are different. An example of the synthetic data (asterisks) used for the inversion (S/N = 10), and reconstructed theoretical signals are presented in Figure 12. All the measurements were employed for inversion with $R = 0.94$ and only those marked by circles for inversion with $R = 0.86$. A good fit is obtained for both the theoretical curves and the model data contaminated by noise, but the solution using $R = 0.86$ is preferable because of the smaller number of measurements.

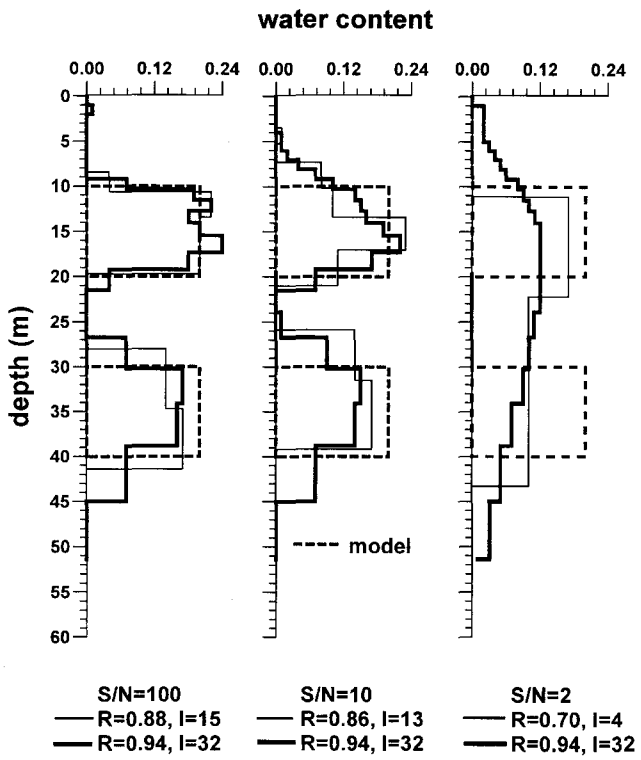

FIG. 11. Results of the inversion of synthetic data with random noise added.

Field data inversion

Field experiments were carried out both in Russia and in France over well-known aquifers.

At the test site near Novosibirsk, Russia, an aquifer consisting of medium- to coarse-grained sand is located approximately between 20 and 40 m. The water is fresh, and the resistivity of the first 50 m is around 50 ohm-m. The resistivity was measured by the dc resistivity method. A more conductive layer of clay below 50 m did not significantly influence the measured normal moveout (NMR) signal. The measurements were performed near borehole N 37. The lithological log of the borehole and the inversion results are presented in Figure 13. The inclination of the geomagnetic field at the test area is approximately 72° and S/N = 48. According to our experience, this level of S/N is high and the inversion results should therefore be reliable. The optimal number of basis functions was found to be 14 ($J = 14$), and hence 14 measurements were chosen ($I = 14$). Inversion with $J = 14$, $I = 14$ is shown by the dashed line in Figure 12. Inversion with $J = 27$, $I = 28$ was also performed (solid line) to demonstrate that there is no fundamental difference between the two solutions. A water-saturated zone detected by NMR between 20 and 50 m coincides quite well with the lithological log. As the practical accuracy of field measurements does not allow accurate detection of layer boundaries at depths below 40 m, it is hard to determine the exact location of the base of the aquifer. Experimental data and reconstructed theoretical signals are presented in Figure 14. They coincide well and demonstrate the accuracy of the inversion. The measurements employed in the optimal inversion ($J = 14$, $I = 14$) are marked with circles.

At the test area of St-Cyr-en-Val, France, three aquifers were determined during a BRGM geological study. The upper aquifer consists of a stratum of mixed gravel, sand, and clay, approximately 20–25-m thick. The two others consist of water-saturated karst limestone separated by a sandstone layer

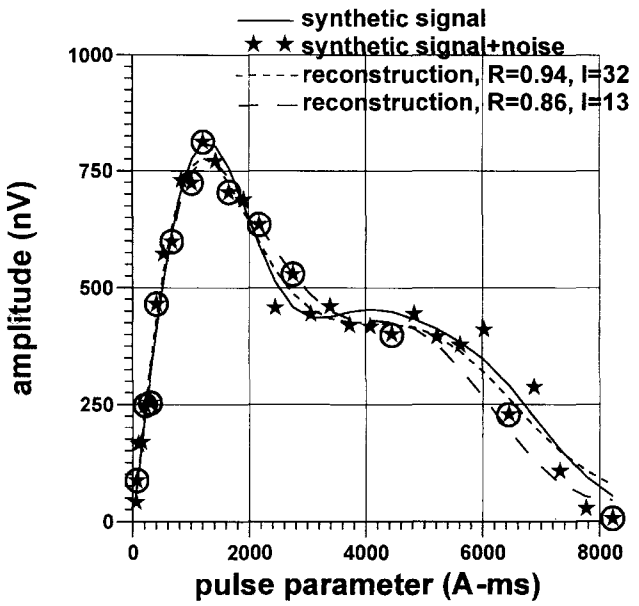

FIG. 12. Synthetic data with random noise added (S/N = 10), and the NMR signal amplitudes reconstructed from inversion results for the model shown in Figure 11.

at a depth of 50–60 m. The total thickness of the karst limestone aquifers is about 40–50 m and the average porosity is approximately 10%. Water transmissivity of the karst limestone is around 0.28 sq.m/s. The lithological log of borehole N 268, situated approximately 600 m from the NMR test site, the surface dc resistivity method and the NMR data interpretation results are presented in Figure 15. The dc resistivity measurements performed did not indicate any significant difference between the borehole site and the NMR test site itself. The noise estimation was S/N = 7.8. For the inversion, we used an optimal ($J = 10$, $I = 10$, dashed line) and a nonoptimal ($J = 27$, $I = 27$, solid line) set of measurements. The matrix $\underset{\sim}{\mathbf{A}}$ was calculated using the subsurface resistivity vertical distribution data, measured by the dc resistivity method. The geomagnetic field inclination is equal to 62°. Once again, both solutions were found to be similar. The observed difference between the depth of the detected shallow aquifer and the water table may be explained by noise influence on the interpretation results. Because of the lack of a borehole at the test site itself, it is not possible to verify the exact depth and thickness of this shallow, fairly irregular aquifer. The limestone aquifer between 28 and 52 m is quite extensive throughout the area, and is well-detected by NMR. No water was found below 60 m. This negative result may be explained easily by the existence of an electrically conductive shallow layer (approximately 25 m thick, with a resistivity of 9 ohm-m), whose screening effect decreases the depth of investigation. Reconstructed theoretical signals from detected aquifers (Figure 16) correspond well with the true measurements, considering the fairly large dispersion of the noise-contaminated data. The measurements used for the inversion with $J = 10$, $I = 10$ are marked by circles.

CONCLUSIONS

The algorithm of measurement optimization for the surface NMR method, with the correlation coefficient between the kernel vectors as a parameter of the discretization, makes it possible to determine the reasonable minimum number of measurements, and therefore, minimize duration of field measurement without a loss of information for a given S/N. Inversion based on the Tikhonov regularization method is stable within a wide range of signal to noise ratios.

Depth of investigation and vertical resolution depend on the electrical conductivity of the subsurface. Where conductive layers are present, the screening effect, which attenuates the NMR signal, results in a decrease in the depth of investigation. For example, with a 100-m-diameter circular antenna, a vertical geomagnetic field of $\alpha = 90°$, and a Larmor frequency of $\omega_0/2\pi = 2500$ Hz, the maximum depth of investigation varies from 200 m for free space to 48 m for a 1 ohm-m half-space.

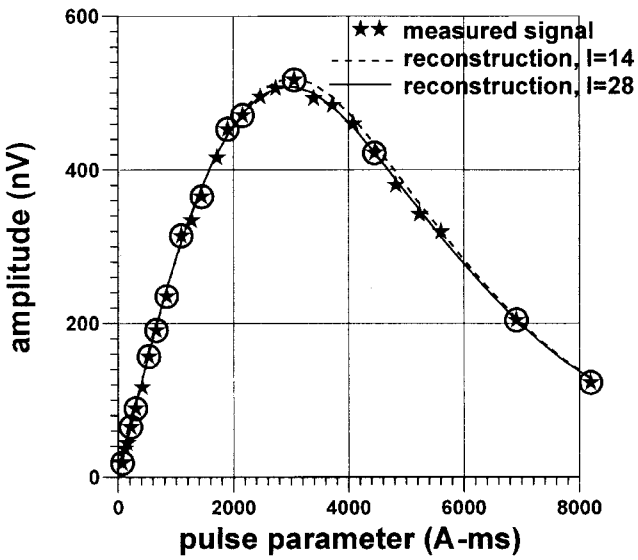

FIG. 14. The NMR field data (asterisks) from the test site at Novosibirsk plotted with the theoretical reconstruction based on inversion results.

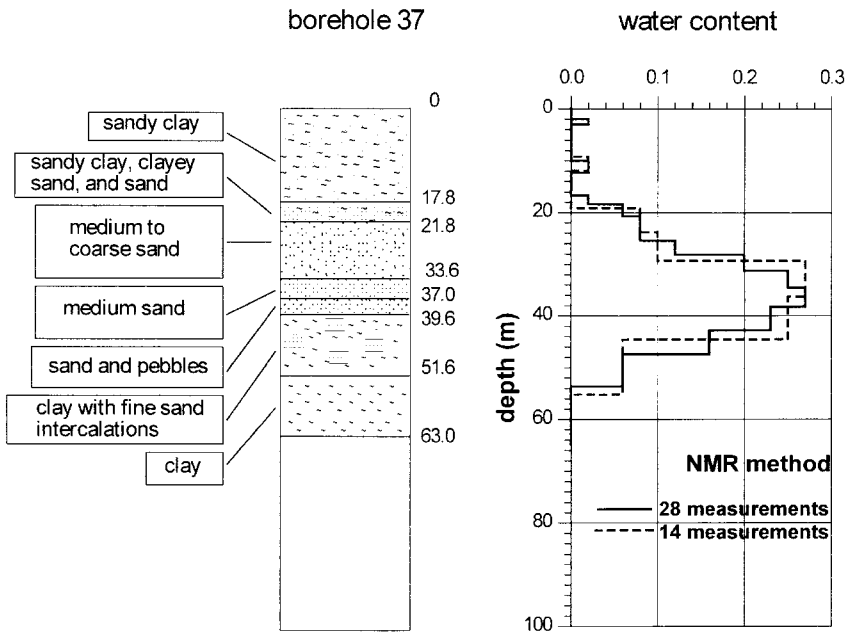

FIG. 13. Lithological log of borehole N 37 near Novosibirsk together with the results from inversion of the NMR field data set.

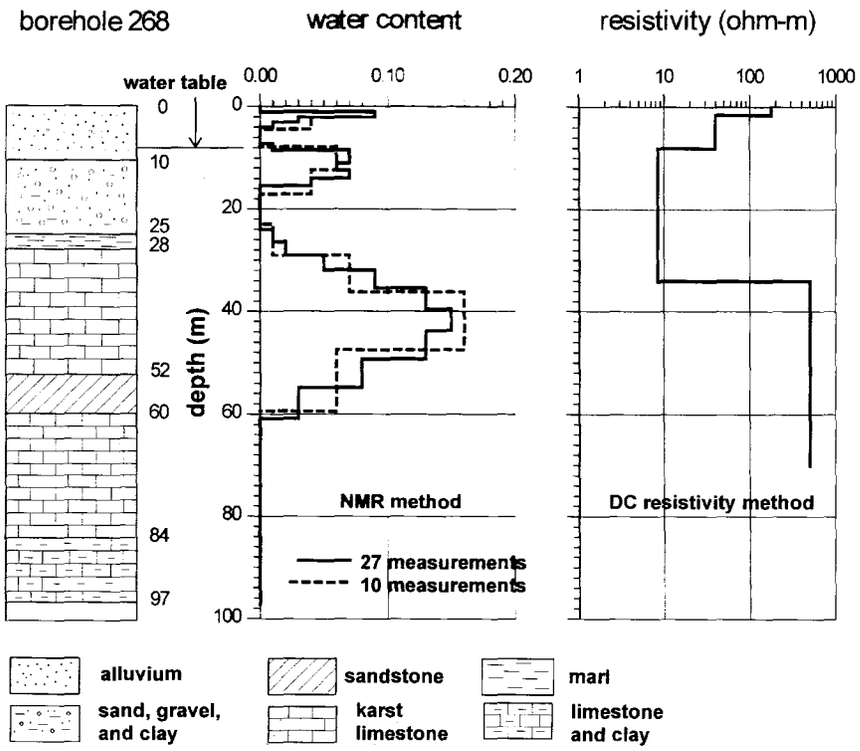

FIG. 15. Inversion results from NMR and dc resistivity soundings and a lithological log from a nearby borehole (N 268) at St-Cyr-en-Val.

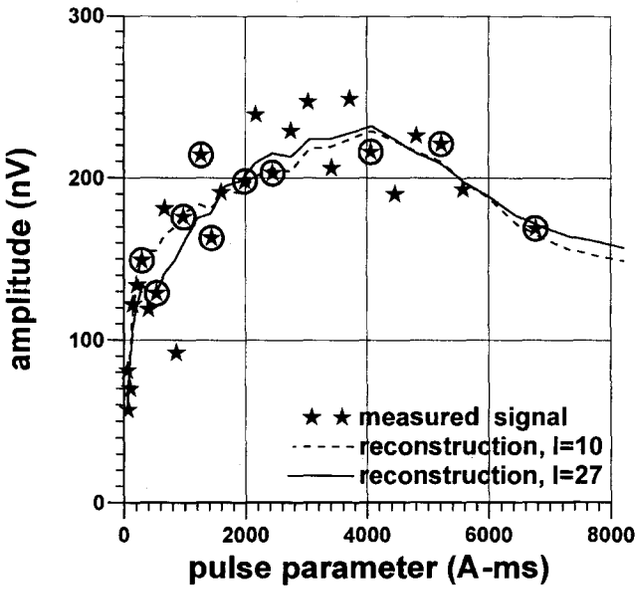

FIG. 16. The NMR field data (asterisks) from the test site at St-Cyr-en-Val plotted with the theoretical reconstruction based on inversion results.

Within the resistivity interval 10 to 100 ohm-m, the maximum depth of investigation varies from 110 to 170 m, respectively.

ACKNOWLEDGMENTS

The authors would like to acknowledge the assistance of BRGM, France, for the results of the NMR field tests and the geological data, and thank A. Straub, A. Beauce and P. Valla for fruitful discussions which helped to improve the paper.

REFERENCES

Goldman, M., Rabinovich, B., Rabinovich, M., Gilad, D., Gev, I., and Schirov, M., 1994, Application of integrated NMR-TDEM method in groundwater exploration in Israel: J. Appl. Geophys., **31**, 27–52.

Lieblich, D. A., Legchenko, A., Haeni, F. P., and Portselan, A., 1994, Surface nuclear magnetic resonance experiments to detect subsurface water at Haddam Meadows, Connecticut: Proc. of Symp. on Application of Geophysics to Engineering and Environmental Problems: Environ. and Eng. Geophys. Soc. **2**, 717–736.

Morozov, V. A., 1966, On the solution of functional equations by the method of regularization: Soviet Math. Doklady, **7**, 414–417 (English translation).

Schirov, M., Legchenko, A., and Creer, G., 1991, New direct noninvasive groundwater detection technology for Australia: Expl. Geophys., **22**, 333–338.

Shushakov, O. A., 1996, Groundwater NMR in conductive water: Geophysics, **61**, No. 4, 998–1006.

Stoer, J., and Bulirsch, R., 1980, Introduction to numerical analysis: Springer–Verlag, Berlin.

Tarantola, A., 1987, Inverse problem theory. Methods for data fitting and model parameter estimation: Elsevier Science Publ. Co., Inc.

Tikhonov, A., and Arsenin, V., 1977, Solution of ill-posed problems: John Wiley & Sons, Inc.

Trushkin, D. V., Shushakov, O. A., and Legchenko, A. V., 1993, Modulation effects in non-drilling NMR in the earth's field: Appl. Magnetic Resonance, **5**, 399–406.

——— 1994, The potential of a noise-reducing antenna for surface NMR ground water surveys in the earth's magnetic field: Geophys. Prosp., **42**, 855–862.

——— 1995, Surface NMR applied to an electroconductive medium: Geophys. Prosp., **43**, 623–633.

Twomey, S., 1974, Information content in remote sensing: Appl. Opt., **13**, No. 4, 942–945.